ESR and XPS Investigation of a Mo-ηAl_2O_3 Model Catalyst System and Its Interaction with Adsorbed Aromatics

L. Petrakis,* P. L. Meyer, and T. P. Debies

Gulf Research and Development Company, Pittsburgh, Pennsylvania 15230 *(Received September 27, 1979)*

Publication costs assisted by Gulf Research and Development Company

Molybdena–alumina is a chemically interesting model of several industrially significant catalysts, and, as a result, it has received considerable attention. In this paper we report on certain electron spin resonance (ESR) investigations through which we have attempted to develop data in a systematic fashion for the clearer understanding of the behavior of this system. We have quantitatively determined the intensity of the Mo(V) signal, its **g** tensor components, line shape, and line width, and the dependence of these parameters on support, thermal treatments, and adsorption of various aromatics and heteroaromatics. Computer fitting of the spectra has been carried out for a more precise definition of the spectral parameters of the Mo(V) signal. X-ray photoelectron spectroscopy (XPS) has also been utilized to determine the distribution of molybdena valences.

I. Introduction

Molybdena–alumina is a model catalyst system which has attracted considerable attention over the past several years. This system is quite interesting not only because of its varied chemical behavior but also because it serves as a pertinent model for many industrial catalysts.[1-5] A considerable number of the studies of this system have been directed to understanding the distribution of the molybdenum valences and also to determining the crystal fields of the various molybdenum species. Electron spin resonance (ESR) and X-ray photoelectron spectroscopy (XPS) have been used extensively along with other spectroscopies for investigations in this area. The attraction of the first two techniques, especially when used in combination, is that they have the potential for both quantitative and qualitative determinations of the various Mo valences. Although molybdenum is incorporated into the support as a hexavalent species, it is well-known that the support, as well as the various treatments and modes of preparation, can have important effects on the distribution of molybdenum valences. XPS has been used to determine the distribution and binding energies of molybdenum valences in the surface layers of the catalyst,[6-9] and ESR has been used to study the distribution and crystal field structure of Mo(V) in the bulk catalyst.[4,5,10-20] Both Mo(III) and perhaps Mo(IV) could also be detected by ESR.

A quantitative comparison of ESR and XPS analyses of molybdena–alumina systems reveals considerable differences. These differences have been attributed to the different ranges of the two techniques (surface vs. bulk) and also to the existence of more than one Mo(V) species.[21] The exact nature of the Mo(V) site appears uncertain. It has been argued that it is due to Mo(VI) in O_h symmetry which, upon reduction, loses oxygen to form Mo(V) in a square pyramidal coordination. It has also been argued that the Mo(V) signal originates from species occupying tetragonally distorted T_d sites.[22]

Significant and chemically interesting as the molybdena–alumina system is, and despite the widespread attraction that it has received, the system is not completely understood. The ESR results reported earlier by various workers appear, for the most part, to have been done quite carefully. Yet, there are widespread differences reported, even for apparently not too dissimilar systems. For example, the ESR-determined Mo(V) concentration varies by three orders of magnitude. This widespread variation is surely a reflection of the great complexity of the molybdena–alumina system. Quite possibly, these systems are different from each other, their subtle but significant differences resulting from a variation in the preparation procedures. This point is rather difficult to ascertain with any degree of confidence because the literature does not provide the same information for all the systems. Therefore, in this paper, we are concerned with one system, which we describe in some detail. We undertook this work to systematically develop ESR and XPS data that will contribute to a more complete understanding of this system. In this study of a 9% by weight Mo-ηAl_2O_3 catalyst and its interaction with adsorbed aromatics and heteroaromatics, we will investigate (a) the effects of support, thermal treatments, and adsorption of aromatics or heteroaromatics on the molybdenum species and (b) the spectral parameters that quantitatively characterize the site of the Mo(V) species.

II. Experimental Procedures

A. Preparation of the Catalyst Samples. Batches of the 9% Mo-ηAl_2O_3 catalyst were typically prepared as described earlier.[16] Samples of the model catalyst were then treated by one of the following thermal treatments.

(1) Two-Hour Evacuation and Calcination (2-h EC). A 0.3-g sample of the 9% Mo-ηAl_2O_3 catalyst was weighed, placed in a reaction tube, and heated to 500 °C in a vacuum of about 10^{-3} Pa (10^{-5} torr). After 2 h at 500 °C, the reaction tube was removed from the vacuum line and heater, opened to the air, and cooled to 200 °C. Two mL of an aromatic or heteroaromatic in C_6H_{12} was then added and the reaction tube immediately closed off from the air. The reaction tube was shaken for about 0.5 min to ensure adequate mixing of the catalyst and solution and then returned to the vacuum line. The catalyst was evacuated for 0.5 h after it appeared to be dry. While still under vacuum, the catalyst was transferred to a Pyrex ESR side-arm tube. The ESR tube was sealed off and stored in the dark. Sufficient quantities of sample were prepared so that the ESR sample tube was filled well beyond the ends of the ESR spectrometer cavity.

(2) Four-Hour Evacuation and Calcination (4-h EC). As in the previous procedure, samples prepared by this technique were heated for 2 h at 500 °C under vacuum.

0022-3654/80/2084-1020$01.00/0

TABLE I: Definition of Terms in Experimental Procedures

"unsupported samples"	MoO_2, MoO_3
"supported samples"	9% Mo–ηAl_2O_3
"thermal treatment"	heating *after* preparation
2-h EC	evacuated 2 h at 500 °C
4-h EC	evacuated 2 h at 500 °C, heated in air 2 h at 500 °C
2-h H_2 Red.	heated in flowing H_2 2 h at 500 °C
"blank" samples	neither solvent nor probes added after "thermal treatment"
"solvent only" samples	2 mL of solvent added following "thermal treatment"
samples with "probes" (adsorbed species)	aromatics or heteroaromatics added to sample 2 mL of 10^{-2} M solutions of probe in C_6H_{12} added following "thermal treatment"

However, the 4-h EC samples were heated for an additional 2 h at 500 °C in air. The rest of this procedure is the same as the one outlined above.

(3) *Two-Hour Hydrogen Reduction (2-h H_2 Red.).* These samples were heated for 2 h at 500 °C in dried, flowing H_2. The rest of this procedure is the same as in (1), above.

Table I summarizes the types of samples investigated and defines the terms used to describe the various treatments.

B. ESR and XPS. A Varian ESR spectrometer (Model V-4600) operating at 9.5 GHz with 100-kHz field modulation and a 12-in. magnet was used to obtain spectra for the determination of g values. 1,1-Diphenyl-2-picrylhydrazyl (DPPH) was used for calibration. A dual-cavity Varian ESR spectrometer (Model V-4500) with 400-Hz and 100-kHz cavities and a 9-in. magnet was used to obtain spectra for the determination of absolute intensities. An ash sample was used as reference. Signal intensities were determined by the "cut-and-weigh method".

A Fortran program was used to simulate ESR spectra.[23] Basically, the program requires input parameters which describe the microwave frequency, magnetic field, signal height, choice of the line shape (Gaussian or Lorentzian), and suggested g values and line widths. Line shapes, g values, and line widths were varied until the best fit was obtained. The goodness of fit was determined by superposition of simulated and experimental spectra.

Selected samples were also studied by X-ray photoelectron spectroscopy (XPS). The sealed ESR tubes were placed in a glovebox which was purged with nitrogen before the tubes were opened. The catalyst samples were then sprinkled onto a plate covered with double-backed tape. The plate was fixed to a linear-rotary motion probe, inserted into the XPS spectrometer, and evacuated. Electron spectra were measured with a modified AEI-ES100 spectrometer. Modifications of the electron spectrometer included the addition of a turbomolecular-pumped preparation chamber, ion pumping of the electron energy analyzer, and cryogenic pumping of the target chamber. All spectra were recorded at a vacuum of 10^{-5} Pa (10^{-7} torr). The samples were illuminated by Al Kα X-rays with a power setting of 300 W. Spectral binding energies were calibrated by reference to the C 1s contaminant line.

Binding energies of the Mo(IV) and Mo(V) species were determined by deconvolution, assuming that their respective spectral components would have full-width at half-maximum and spin–orbital doublet separations identical with those of Mo(VI). The binding energy of the Mo(VI) component of thermally treated 9% Mo–ηAl_2O_3 samples is assumed to be identical with that of pure MoO_3. All measured binding energies have an uncertainty of ±0.3 eV. The percentage composition of the various molybdenum species was determined by peak area measurements of the deconvoluted components. All percentage compositions are accurate to within ±10%.

III. Results

A. Distribution of Molybdenum Valences (XPS and ESR). (1) Binding Energies and Signal Intensities of the Molybdenum Species. In an attempt to understand the effect of the support on the distribution of molybdenum valences in 9% Mo–ηAl_2O_3 samples, ESR and XPS spectra of various unsupported MoO_2 and MoO_3 samples were analyzed.

(a) Thermally Untreated and Unsupported MoO_2 and MoO_3. MoO_2 and MoO_3 samples were analyzed by ESR and XPS. There was no thermal treatment of either of these unsupported samples, and ESR analysis did not detect the Mo(V) species in either sample. The MoO_3 spectrum consisted of a single well-resolved Mo 3d doublet which was attributed to Mo(VI). A Mo(VI) $3d_{5/2}$ binding energy of 232.5 eV was recorded in good agreement with literature values.[6,24–26]

The surface layers of MoO_2 oxidize when exposed to air. This resulted in a complex Mo 3d spectrum and caused uncertainty in the measurement of the Mo(IV) binding energy. Deconvolution of this spectrum determined that the binding energy of the Mo(IV) component was 229.5 eV, in good agreement with literature values.[8,25–26]

In the following section, several different types of 9% Mo–ηAl_2O_3 samples were prepared and analyzed by ESR and XPS. Thermally untreated 9% Mo–ηAl_2O_3 samples were considered in addition to samples prepared by all three thermal treatments. The thermally treated samples include "blank" samples where no solvent or probe was added, "solvent only" samples where 2 mL of the solvent was added, and samples containing a "probe" (adsorbed species) where 2 mL of a 10^{-2} M solution of an aromatic or heteroaromatic in cyclohexane was added.

(b) Thermally Untreated 9% Mo–ηAl_2O_3. A sample of 9% Mo–ηAl_2O_3 was prepared by simply evacuating a portion of the catalyst at room temperature. The sample was not exposed to any further thermal treatment, and an ESR analysis did not detect Mo(V). The XPS spectrum consisted mainly of a single peak which binding-energy measurements identified as Mo(VI). A comparison of MoO_3 and thermally untreated catalyst indicates that the thermally untreated 9% Mo–ηAl_2O_3 Mo 3d spectrum is slightly broadened. Also, the minimum between the Mo $3d_{5/2}$ and $3d_{3/2}$ components is not as sharply defined in the 9% Mo–ηAl_2O_3 spectrum as in the spectrum of the unsupported material. This signal broadening may be due in part to the presence of a Mo(V) species. The presence of the Mo(V) species is difficult to determine because (1) only a small amount of Mo(V), if any, may be present and (2) the binding energy of the Mo(V) component is very close to that of the Mo(VI) and Mo(IV) components, making it difficult to resolve the signals.

(c) Thermally Treated 9% Mo–ηAl_2O_3. (i) "Blank" Samples. We have already mentioned that no Mo(V) signal was observed by ESR in 9% Mo–ηAl_2O_3 samples which had not undergone thermal treatment. Upon thermal treatment, however, an ESR Mo(V) signal was detected in the 9% Mo–ηAl_2O_3 samples even when no solvent or probe was added. Such samples (without probe or solvent) are referred to as "blanks". ESR results indicated that approximately 1.0% of the total molybdenum in the sample was present as Mo(V) in both the "blank" 2-h EC samples and in the "blank" 2-h H_2 Red. samples (Table II) and that about 0.1% of the total molybdenum

TABLE II: ESR and XPS Determination of Mo Valences in 9% Mo–η Al_2O_3

	deconvoluted XPS, % signal			ESR, wt %
	Mo-(IV)	Mo-(V)	Mo-(VI)	Mo-(V)[a]
untreated 9% Mo–η Al_2O_3			~100	
2-h EC				
blank			~100	1.0
cyclohexane only			~100	0.7
phenazine			~100	0.7
2,3-benzothiophene			~100	1.0
4-h EC				
naphthalene			~100	0.4
phenazine			~100	0.4
phenothiazine	18	41	41	0.07
phenoxanthin		45	55	0.3
thianthrene			~100	0.8
2,3-benzothiophene			~100	0.6
2-h H_2 Red.				
blank		54	46	0.6
cyclohexane only	18	37	45	0.6
naphthalene	35	30	35	0.6
phenazine	22	42	53	0.6
phenothiazine	22	29	49	0.7
phenoxanthin	27	32	41	0.7
thianthrene		53	47	0.6
2,3-benzothiophene		53	47	0.6

[a] Based on formula weights of reactants.

was present as Mo(V) in the "blank" 4-h EC samples (Table III).

The XPS Mo 3d spectrum of the "blank" 2-h EC sample was quite similar to the spectrum of the starting material, i.e., thermally untreated 9% Mo–ηAl_2O_3. The XPS spectrum of both samples contained a single main component which binding-energy measurements identified as Mo(VI). Like the spectrum of thermally untreated 9% Mo–ηAl_2O_3, the spectrum of the "blank" 2-h EC samples is slightly broadened, and the Mo 3d doublet was not as well resolved as in the spectrum of the MoO_3 sample. Again, this may indicate the presence of a small Mo(V) component in the "blank" 2-h EC sample.

The XPS Mo 3d spectrum of a "blank" 2-h H_2 Red. sample had a definite low field broadening, indicating that some of the molybdenum had been reduced by this thermal treatment. Deconvolution of the XPS spectrum determined the surface composition of this sample to be 46% Mo(VI) and 54% Mo(V) (Table II).

(*ii*) "*Solvent (Cyclohexane) Only*" *Samples.* Other thermally treated samples were prepared where only the solvent was added. Mo(V) ESR signals were detected in each sample, regardless of the thermal treatment used. ESR intensity measurements determined the fraction of the total molybdenum present as Mo(V) in samples prepared by each thermal treatment: 0.7% for the 2-h EC samples, 0.2% for the 4-h EC samples, and 0.6% for the 2-h H_2 Red. samples (Table III).

The XPS Mo 3d spectrum of the 2-h EC "solvent only" sample was similar to the spectra of both the "blank" 2-h EC sample and the thermally untreated 9% Mo–ηAl_2O_3 sample which were reported earlier. Again, the main component of the XPS spectrum was the Mo(VI) doublet. Since the 2-h EC "solvent only" spectrum was broadened and not well resolved compared to the MoO_3 spectrum, the presence of a small Mo(V) component is a possibility.

The XPS spectra of the "solvent only" H_2 Red. samples were broad envelopes, obviously containing several components, and deconvolution showed that more than half

TABLE III: Average ESR Signal Intensities of Mo(V) Signals in 9% Mo–η Al_2O_3 Samples[a]

	2-h EC	4-h EC	2-h H_2 Red.
blank	2.5	0.5	3.7
cyclohexane only	3.9	1.4	3.7
toluene only	NA[b]	4.1	3.8
toluene	NA[b]	1.7	3.7
naphthalene	4.2	2.2	3.3
anthracene	4.5	2.9	3.5
phenanthrene	4.1	3.4	4.1
azulene	5.4	4.1	2.9
phenazine	4.0	2.5	3.2
phenothiazine	2.4	0.4	3.8
phenoxanthin	3.9	1.7	4.3
phenoxazine	2.6	0.4	4.4
thianthrene	5.2	4.7	3.6
thiophene	2.8	2.3	3.7
2,3-benzothiophene	5.7	3.5	3.5
dibenzothiophene	4.4	2.6	3.5
acridan	5.3	NA[b]	3.3
acridine	3.4	NA[b]	3.7
xanthene	6.4	NA[b]	3.3

[a] ($\times 10^8$ spins/g of catalyst). Signal intensities represent average from up to four different samples. Maximum and minimum absolute errors are, respectively, 1.4×10^{18} and 0.01×10^{18} spins/g of catalyst. Thermal treatments and sample types are defined in Table I. [b] NA = not available.

of the original Mo(VI) had been reduced. XPS determined the surface composition to be 45% Mo(VI), 37% Mo(V), and 18% Mo(IV) (Table II).

(*iii*) *Samples with "Probes" (Adsorbed Species).* When samples of 9% Mo–ηAl_2O_3 were thermally treated by any of the three procedures (Table I) and a probe solution was added, Mo(V) signals were always observed by ESR. The intensity of these Mo(V) signals was found to be a function of the adsorbed species, the heating time, and the particular thermal treatment. Although the 2-h H_2 Red. Mo(V) signal intensities were relatively unaffected by the various aromatics and heteroaromatics added to the catalyst, the EC Mo(V) signal intensities were found to vary as a function of the particular adsorbed species.

A comparison of the Mo(V) ESR signal intensities from both of the EC procedures (2-h and 4-h) showed that the latter procedure generally produced a smaller Mo(V) signal intensity (Table III). The type of thermal treatment is another factor influencing the intensity of the Mo(V) signals in the 9% Mo–ηAl_2O_3 catalyst samples. Table III shows that the Mo(V) EC signal intensities varied over a much wider range than did the H_2 Red. signal intensities. For example, the Mo(V) signal intensities ranged from 2.4×10^{18} to 6.4×10^{18} spins/g of catalyst in the 2-h EC samples and from 0.4×10^{18} to 4.7×10^{18} spins/g of catalyst in the 4-h EC samples. In contrast, the 2-h H_2 Red. Mo(V) signal intensities were only found to vary from 2.9×10^{18} to 4.4×10^{18} spins/g of catalyst.

XPS analysis of selected thermally treated 9% Mo–ηAl_2O_3 samples with adsorbed species indicated that the distribution of Mo valences also depended on the thermal treatment of the samples and on the particular adsorbed species.

The XPS spectra of the EC samples generally consisted of a single broadened Mo 3d doublet which binding-energy measurements identified as Mo(VI). The following catalyst samples were analyzed by XPS: 2-h EC with phenazine, 2,3-benzothiophene, acridine, or xanthene; and 4-h EC with naphthalene, phenazine, phenothiazine, phenoxanthin, 2,3-benzothiophene, or thianthrene. All the EC Mo 3d XPS spectra were broadened relative to the spectrum of pure, unsupported MoO_3, but most were comparable in

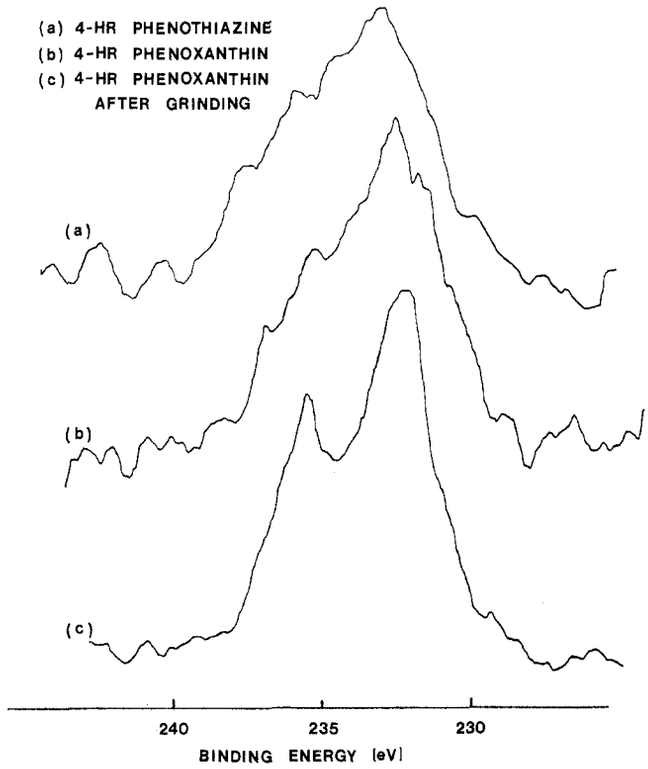

Figure 1. XPS Mo 3d spectra of 9% Mo–ηAl_2O_3 evacuation and calcination (EC) samples: (a) 4-h phenothiazine; (b) 4-h phenoxanthin; (c) same sample as b after grinding by mortar and pestle.

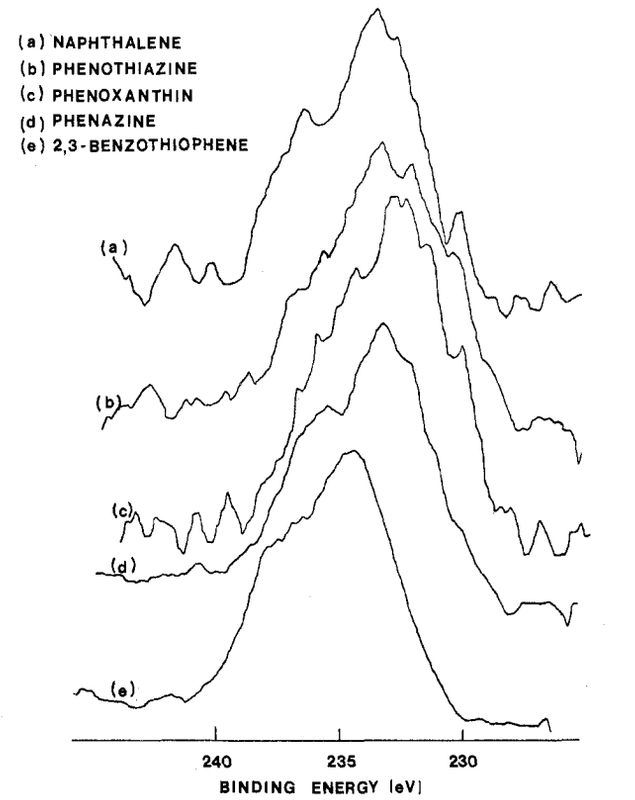

Figure 2. XPS Mo 3d spectra of typical 9% Mo–ηAl_2O_3 2-h H_2-reduced (H_2 Red.) samples: (a) naphthalene; (b) phenothiazine; (c) phenoxanthin; (d) phenazine; (e) 2,3-benzothiophene.

width with the spectrum of thermally untreated 9% Mo–ηAl_2O_3. Although the 2-h and 4-h EC samples could be differentiated on the basis of their ESR Mo(V) signal intensities, these samples were not distinguishable by XPS. Both 2-h and 4-h EC samples appeared to contain mainly Mo(VI) on the basis of XPS analysis. Since these XPS signals were slightly broadened and not so well resolved as the XPS MoO_3 signal, a small Mo(V) component could also be present. However, it was not possible to accurately determine this component by deconvolution.

The XPS spectra of two 4-h EC samples, phenoxanthin and phenothiazine, were exceptions to the usual signal shape. Instead of a Mo(VI) doublet, these samples had broad and featureless XPS spectra (Figure 1, a and b). A possible explanation for the observed spectra might be the presence of more than one molybdenum species. Deconvolution determined the apparent surface composition of the phenoxanthin sample to be 55% Mo(VI) and 34% Mo(V), whereas the phenothiazine sample contained 41% Mo(VI), 41% Mo(V), and 18% Mo(IV) (Table II). An alternative explanation for the spectra (Figure 1, a and b) is that an abnormally high amount of heteroaromatic might be adsorbed on the catalyst surface. Mechanical grinding of the catalyst pellets by mortar and pestle was used to expose the subsurface layers of the catalyst. Whereas grinding other EC or H_2 Red. samples did not result in any significant changes in signal shape or intensity, mechanical grinding of the phenoxanthin sample had two effects: (1) the spectral intensity of the molybdenum signal was increased by a factor of seven and (2) a spectrum of a single, broadened Mo(VI) doublet was obtained (Figure 1, b and c). Perhaps this single Mo species represents the spectrum of unreacted material or perhaps it represents the Mo spectrum unobscured by adsorbed species. It was interesting to note that the ESR spectra of these two samples were also exceptional. They consisted of unusually large radical cation signals and unusually small Mo(V) signals (Table III).

The 2-h H_2 Red. XPS spectra of thermally treated catalyst samples with adsorbed species were quite different in appearance from the corresponding EC spectra. The following 2-h H_2 Red. samples were analyzed: naphthalene, phenazine, acridine, phenothiazine, phenoxanthin, thianthrene, and 2,3-benzothiophene. Although most of the EC spectra contained mainly a single Mo species, the 2-h H_2 Red. spectra were broader and the individual components were not readily apparent (Figure 2). Features common to most of the 2-h H_2 Red. spectra included a low binding-energy shoulder attributed to Mo(IV) and a second shoulder approximately 1 eV below the curve maximum which was assigned to Mo(V). The observed spectral maximum is due to the overlap of centroids and, therefore, does not agree with the binding energy of any pure species. Deconvolution of the 2-h H_2 Red. samples yielded the following distribution of Mo valences on the sample surfaces: 0–35% Mo(IV), 29–53% Mo(V), and 35–53% Mo(VI) (Table II). When H_2 Red. 9% Mo–ηAl_2O_3 samples containing adsorbed species were compared with 9% Mo–ηAl_2O_3 samples which had not been exposed to any thermal treatment, it was found that about half of the original Mo(VI) was reduced to lower valences by the 2-h H_2 Red. thermal treatment. None of the 2-h Red. samples analyzed by XPS contained any molybdenum species lower than the Mo(IV), and only two samples, thianthrene and 2,3-benzothiophene, lacked this species.

(2) *Line Widths, g Values, and Signal Shapes of the Mo(V) ESR Spectra.* (a) *Experimental ΔH_{pp} and g Values.* In order to characterize the environment and crystal field of the ESR Mo(V) species, the following spectral parameters were examined in some detail: the peak-to-peak line width (ΔH_{pp}), the apparent g value, and the line shape.

ΔH_{pp} values were measured for samples prepared by all three thermal treatments and are shown in Table IV. The ΔH_{pp} values are defined as the distance in gauss between

TABLE IV: ESR Mo(V) Signals: Line Width (ΔH_{pp}) in Gauss[a]

	2-h EC	4-h EC	2-h H_2 Red.
blank	73.5	49.8	80.7
cyclohexane only	58.1	43.9	78.9
toluene only	NA[b]	NA[b]	NA[b]
toluene	NA[b]	43.7	78.0
naphthalene	59.0	44.8	77.1
anthracene	67.8	NA[b]	77.5
phenanthrene	71.9	47.9	79.3
azulene	72.4	61.1	75.0
phenazine	56.9	50.8	77.6
phenothiazine	50.3	21.1	76.0
phenoxanthin	60.5	44.2	78.5
phenoxazine	56.7	37.6	80.6
thianthrene	69.0	NA[b]	79.3
thiophene	51.8	44.1	79.9
2,3-benzothiophene	69.4	51.6	81.5
dibenzothiophene	59.7	45.4	80.1
acridan	78.2	NA[b]	80.6
acridine	57.0	NA[b]	80.9
xanthene	68.8	NA[b]	NA[b]

[a] ΔH_{pp} is defined as the distance in gauss between slope extrema. ΔH_{pp} are averages from up to four different samples. Absolute errors ranged from ±0.4 to ±7.3 G, with typical relative errors of ±4%. See Table I for definition of treatments. [b] NA = not available.

the maximum and minimum points of the first-derivative spectrum. This procedure was used for both isotropic and anisotropic spectra. The values shown in Table IV represent the average ΔH_{pp} value from up to four different samples. The absolute uncertainties of the ΔH_{pp} values range from a low of ±0.4 G to a maximum of ±7.3 G. The relative uncertainty is typically ±4%.

The line widths of the Mo(V) signals were found to be noticeably affected by the particular thermal treatment. In Table IV it is evident that a wide range of ΔH_{pp} values was found among the EC samples: from 50 to 76 G for the 2-h samples and from 21 to 62 G for the 4-h samples. In contrast, ΔH_{pp} values of the 2-h H_2 Red. samples covered only a small range of values, from 73 to 83 G. ΔH_{pp} was always greater in the 2-h EC case then in the corresponding 4-h case, and the 2-h H_2 Red. samples had the largest ΔH_{pp} values of all three techniques. These results are in agreement with earlier work by Seshadri and Petrakis.[16]

Table V presents the apparent g value (g_{av}) of the Mo(V) signal from samples prepared by each of the thermal treatments. The apparent g value is defined as the point halfway between the slope extrema of the first-derivative spectrum. This procedure was followed even with some clearly anisotropic spectra which possessed distinct high-field shoulders. The g values in Table V are the averages of g values calculated from up to four different samples. The maximum observed absolute uncertainty in g_{av} values was ±0.00191 (from the same sample which had the maximum uncertainty in ΔH_{pp} values in Table IV). However, the uncertainty in g values was more typically ±0.0007, with the minimum uncertainty being ±0.00005.

The apparent g value of the Mo(V) ESR signals in Table V was calculated by assuming that the DPPH g value = 2.00360. The g values of the Mo(V) signals were found to be affected by the particular adsorbed species and the thermal treatment of the catalyst. Again, as with the ΔH_{pp} values, the EC Mo(V) g values varied over a wider range than did the H_2 Red. g values. The EC g values varied from 1.930 to 1.938, whereas the H_2 Red. g values were found in a much smaller spread, from 1.930 to 1.932. Also, the EC g values appeared to vary similarly as a function of the different aromatics and heteroaromatics, whereas

TABLE V: g Values of Mo(V) ESR Signals[a]

	2-h EC	4-h EC	2-h H_2 Red.
blank	1.93187	1.93674	1.93171
cyclohexane only	1.93484	1.93769	1.93234
toluene only	NA[b]	NA[b]	NA[b]
toluene	NA[b]	1.93764	1.93203
naphthalene	1.93478	1.93706	1.93140
anthracene	1.93289	NA[b]	1.93222
phenanthrene	1.93172	1.93661	1.93123
azulene	1.93148	1.93260	1.93012
phenazine	1.93335	1.93509	1.93039
phenothiazine	1.93845	1.93745	1.93186
phenoxanthin	1.93537	1.93713	1.93218
phenoxazine	1.93803	1.93736	1.93126
thianthrene	1.93345	1.93454	1.93193
thiophene	1.93609	1.93765	1.93163
2,3-benzothiophene	1.93161	1.93623	1.93166
dibenzothiophene	1.93359	1.93652	1.93153
acridan	1.92850	NA[b]	1.93188
acridine	1.93292	NA[b]	1.93060
xanthene	1.93012	NA[b]	NA[b]

[a] The g value was defined as the point halfway between slope extrema. Averages of g values from up to four separate samples are shown. Absolute errors ranged from ±0.00005 to ±0.00191 with typical absolute errors of ±0.00070. See Table I for definition of sample types and thermal treatments. [b] NA = not available.

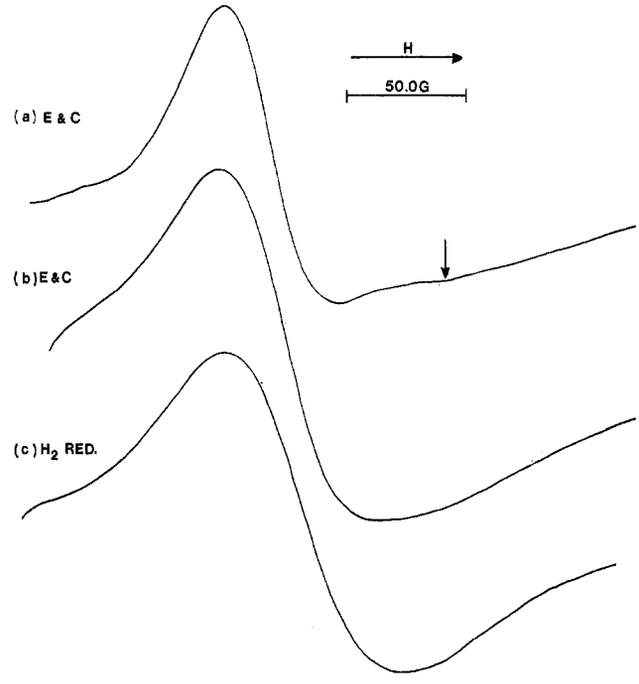

Figure 3. Mo(V) ESR spectral line shapes: (a) an example of the first derivative signal of some evacuation and calcination samples which have a shoulder on the high-field side of the high-field peak; (b) an example of another typical evacuation and calcination line shape; (c) a line shape representative of all H_2-reduced samples.

the H_2 Red. samples were much less affected by the presence of a particular probe.

Another striking difference between the EC samples and the H_2 Red. ones was the actual shape of the ESR Mo(V) first-derivative signal. Whereas all H_2 Red. Mo(V) signals were similar in shape and appeared to be nearly isotropic (Figure 3c), the EC samples were definitely anisotropic (Figure 3, a and b). The high-field half of the EC Mo(V) first-derivative signals was markedly broadened compared to the low-field half. No hyperfine structure due to ^{95}Mo or ^{97}Mo was observed in any of the Mo(V) ESR spectra. These results are similar to the spectral shapes reported by Seshadri and Petrakis,[16] Campadelli and Bart,[27] and Naccache and co-workers[15] in their studies of Mo–ηAl_2O_3

TABLE VI: Δg and $1/\alpha$ Values of Mo(V) Signals in Axially Symmetric Systems

sample	$g_\parallel$	$g_\perp$	g_{av}	Δg	$1/\alpha$	ref
MoO_3						
heated under vacuum	1.875	1.933	1.914	0.058	0.544	30
evacuated	NA[a]	NA[a]	1.943	NA[a]	NA[a]	29
Mo-Al_2O_3						
summary of values from various treatments	1.894-1.922	1.941-1.955	1.926-1.943	0.031-0.052	0.522-0.629	14, 16, 31, this work
aluminonickel molybdenum oxide-Al_2O_3						
6 h 600 °C	1.908	1.936	1.927	0.028	0.703	32
MoO_3-TeO_2	1.876	1.935	1.915	0.059	0.533	33
MoO_3-P_2O_5	1.887	1.940	1.922	0.053	0.540	33
$CdMoO_4$						
2 h in air at 450 °C, evacuated at 400 °C	1.885	1.940	1.922	0.055	0.531	17
$Bi_2(MoO_4)_3$						
evacuated	1.873	1.933	1.913	0.060	0.536	34
$Mo(CO)_6$-Al_2O_3						
prolonged evacuation at room temp	1.905	1.945	1.932	0.040	0.589	28
activated, 400 °C	1.897	1.954	1.935	0.057	0.459	28
$Mo(CO)_6$-SiO_2						
evacuated 19 h, room temp	1.895	1.934	1.921	0.039	0.637	28
evacuated 1 h, 400 °C	1.884	1.948	1.927	0.064	0.459	28
H_2 reduced, 700 °C	1.862	1.955	1.924	0.093	0.337	28
Solution Mo(V)						
acqueous solution of MoO^{3+}, room temp			1.947			35
MoO_3 in HCl, reduced with Zn, Hg			1.950			36

[a] NA = not available.

systems. The difference between the evacuation and calcination signal shapes and the H_2-reduced signal shapes can be attributed to the differing effects that each preparation technique has on the catalyst support.

In the evacuation and calcination samples, the degree of anisotropy was found to depend on the particular aromatic or heteroaromatic molecule used. The use of "blank", "solvent only", naphthalene, phenanthrene, thiophene, 2,3-benzothiophene, and dibenzothiophene gave rise to a second peak in the high-field half of the spectrum in either one or both of the evacuation and calcination procedures (Figure 3a). This feature was not observed in the cases where azulene (4-h), "blank", thianthrene, dibenzothiophene, anthracene, acridan, and phenazine (all 2-h) were used (Figure 3b).

(*b*) *Spectra Fitting Procedures.* In order to provide more definitive information about the Mo(V) species, the spectral shape of this species was investigated through the use of a Fortran ESR simulation program. The overall ESR spectral shape may be affected by the g value anisotropy, the line width of the signal components, the line shape (Gaussian, Lorentzian, etc.), and the hyperfine structure. However, at no time has Mo hyperfine structure been observed unless there has been ^{95}Mo and ^{97}Mo enrichment of the sample. Therefore, the overall spectral shape of the Mo(V) signal should be determined primarily by the first three factors mentioned above.

Table VI presents a survey of the Mo(V) g values reported in the literature for a variety of systems. It can be seen that the difference between $g_\perp$ and $g_\parallel$, Δg, ranges from about 0.028 to about 0.093 for these axially symmetric systems. In addition, the reported ΔH_{pp} values range up to approximately 100 G. With these values as guidelines, we have attempted to determine g values and line-width parameters which best simulate the observed spectra of our model catalysts.

We first used the spectral simulation program to consider the sensitivity of the overall signal shape to systematic variations of ΔH_{pp}, Δg, and line shape. ΔH_{pp} was varied from 10 to 250 G; Δg was varied from completely isotropic ($g_x = g_y = g_z$) to axially anisotropic ($g_x = g_y \neq g_z$) to totally anisotropic ($g_x \neq g_y \neq g_z$); and both Gaussian and Lorentzian line shapes were tested.

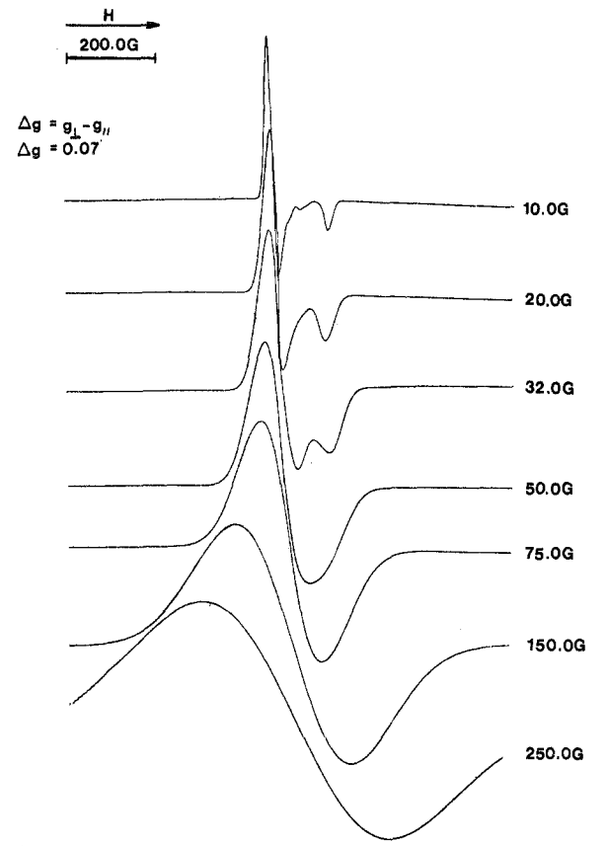

Figure 4. Computer simulations of an axially symmetric Gaussian line shape. The line width varies from 10.0 to 250.0 G while the difference between the components of the g tensor, Δg, remains constant at 0.07.

Figure 4 shows the expected spectral shapes for axially symmetric Gaussian line shapes where ΔH_{pp} = 32 G and Δg is varied from 0.0 to 0.33. Incidentally, $g_\parallel$ must be less than $g_\perp$ in order to locate the shoulder on the high-field peak. Figure 5 is representative of another group of simulated spectra where the line width was varied and Δg remained constant. Also, a Lorentzian line shape is used in Figure 5. One important difference was noted between Gaussian and Lorentzian line shapes. The shoulder on the

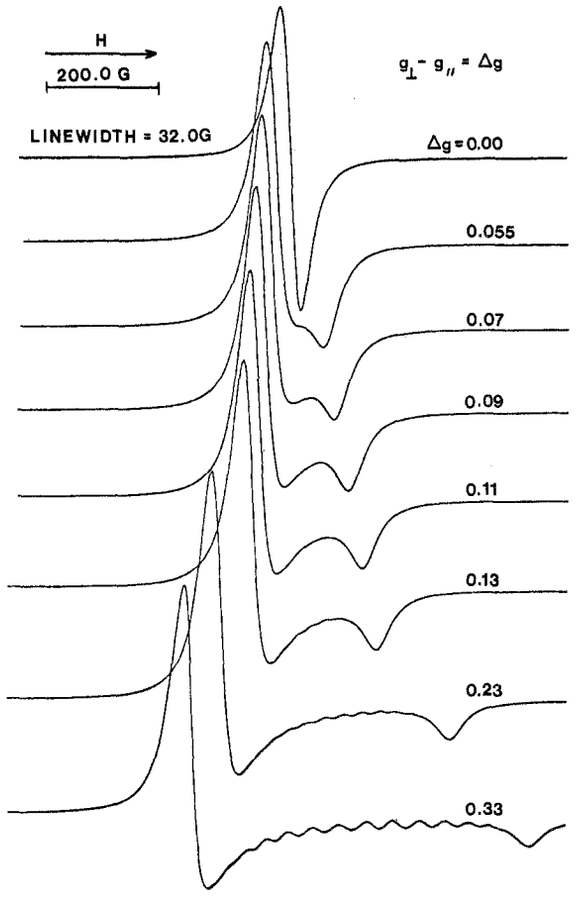

Figure 5. Computer simulations of an axially symmetric Lorentzian line shape; Δg varies from 0.00 to 0.33 while the line width is constant at 32.0 G.

high-field peak, which could be produced with the correct combination of ΔH_{pp} and Δg values, was always located on the low-field side of this peak in Lorentzian simulations. In the Gaussian simulations, this shoulder, if present, was always located on the high-field side of the high-field peak. This subtle difference allows the determination of the line shape of the experimental spectra.

(c) *Comparison of Simulated and Experimental Spectra.* The type of analysis presented above of Δg, ΔH_{pp}, and line shape interations and a consideration of literature values provided the basis for curve fitting the experimental Mo(V) spectra. Computer simulations showed that the EC Mo(V) signals were axially symmetric, having two identical low-field components and one high-field component of the g value tensor with $\Delta g = 0.046$ (Figure 6). As discussed earlier, the EC Mo(V) signals often had a slight shoulder on the high-field side of the high-field peak. We have just seen that the axially symmetric Gaussian line shape can provide the same type of feature whereas the Lorentzian cannot. Fitting the EC spectrum proved not very successful altogether (Figure 6). It is seen that the observed spectrum is intermediate between Gaussian and Lorentzian in the low-field side. The central component is best simulated by Gaussian, whereas the high field is not reproduced very well by either line shape. Computer simulations showed that the 2-h H_2 Red. spectra also possessed axial symmetry with a low-field $g_\perp$ and a high-field $g_{||}$ and $\Delta g = 0.034$ (Figure 7). The computer simulations were able to provide a good fit of the experimental spectrum, both in the central region and on the low-field side. However, the simulations were less successful in fitting the high-field "tail" of the observed spectrum. Both the high- and low-field "tails" of the experimental curve declined

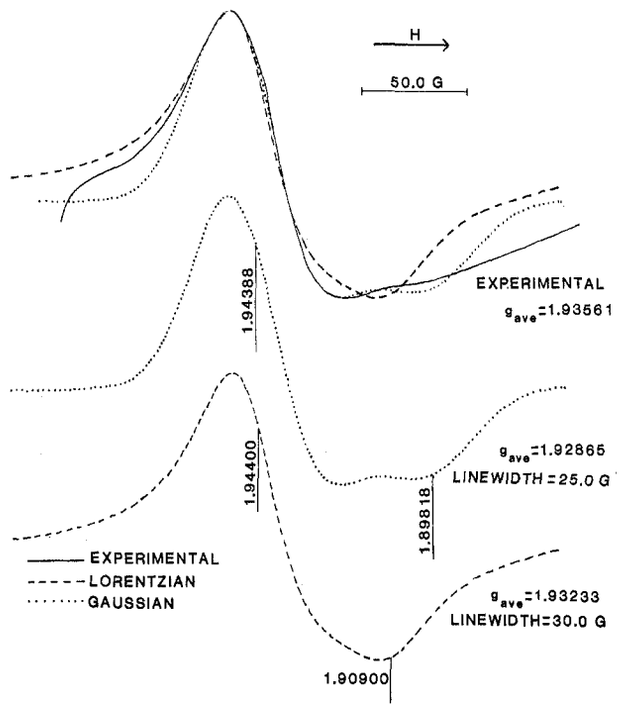

Figure 6. Comparison of experimental and simulated spectra of the Mo(V) ESR signal from a 9% Mo–ηAl_2O_3 2-h evacuation and calcination sample with adsorbed naphthalene.

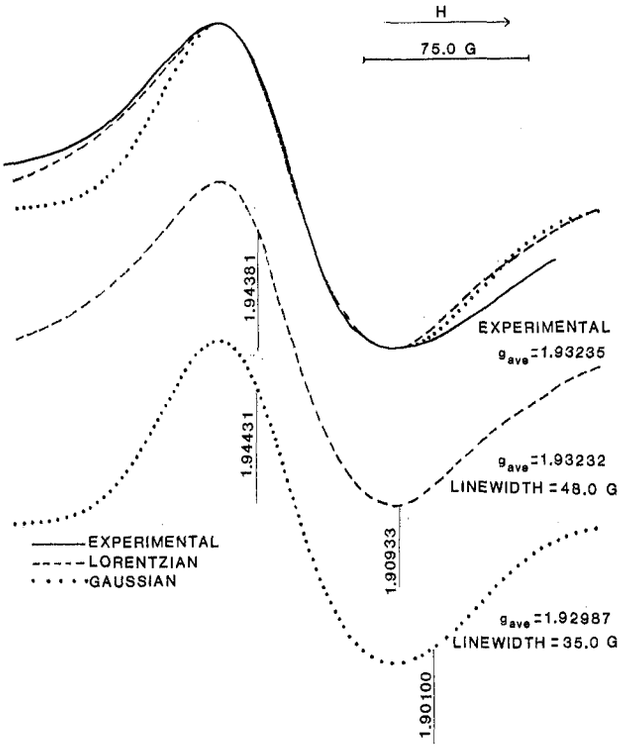

Figure 7. Comparison of experimental and simulated spectra of the Mo(V) ESR signal from a 9% Mo–ηAl_2O_3 2-h H_2-reduced sample with adsorbed cyclohexane.

less rapidly than either the Gaussian or the Lorentzian simulations. Unlike the EC spectra, the best overall fit of the H_2 Red. spectra was provided by a Lorentzian line shape. Computer simulations also verified the existence of wider line widths in the H_2 Red. cases which are responsible along with the smaller Δg values for the symmetric appearance of the H_2 Red. spectra.

Given the many factors that could affect the experimental Mo(V) spectra, it is unrealistic to expect a totally accurate reproduction of the observed spectra with a sim-

TABLE VII: Simulated and Experimental Spectral Parameters of Mo(V) ESR Signals

	parameters for "best fit"				
	line shape	line width, G	g tensor components	g_{av}	exptl[a] g_{av}
evacuation and calcination	Lorentzian		No reasonable fit obtained		
	Gaussian	25	1.94388, 1.94388, 1.89818	1.92865	1.93561
H_2 reduction	Lorentzian	48	1.94381, 1.94381, 1.90933	1.93232	1.93235
	Gaussian	35	1.94431, 1.94431, 1.90100	1.92987	1.93235

[a] Defined as the point halfway between slope extrema (see text).

ulation program that does not include all possible interactions. Among the factors which may prevent the simulation program from completely predicting the observed spectra are the following: a more complicated line-shape function than either pure Gaussian or Lorentzian may be required (e.g., see the low-field "tail" of the experimental spectrum in Figure 6); the existence of the Mo(V) species in a distribution of slightly varying crystal fields; nonuniform dipolar broadening and/or exchange effects, both between the molybdenum dipoles and the cations; possible anisotropic relaxation effects in these polycrystalline samples and contributions from hyperfine interactions (even though unresolved) due to nonzero nuclear spins; and quite likely a wide spectrum of crystal field sites that even prevent the observation of some of the Mo(V) signals.[21]

The best fit obtained is for H_2 Red. samples, which have the more consistent parameters from sample to sample (Figure 7 and Table VII). The Mo(V) evacuation and calcination sample has an experimental $g_{av} = 1.93561$. The best Gaussian fit by computer simulation resulted in $g_{av} = 1.92865$ with $g_\perp = 1.94388$ and $g_\parallel = 1.89818$. The line width was determined to be 25 G. The experimental g_{av} of a H_2-reduced Mo(V) signal was calculated to be 1.93235, and the best Lorentzian simulation resulted in a value of $g_{av} = 1.93232$. Components of the simulated **g** tensor were determined to be 1.90933 and 1.94381, and the line width was 48 G.

The Mo(V) signal shapes from these first approximations may be compared with those obtained by Campadelli and Bart.[27] Using a least-squares procedure and taking into account g values, line widths, and line shapes, they determined that the Mo(V) ESR signals of outgassed (2 h in He at 500 °C) or reduced (2 h in He at 500 °C, 5 h in He/H_2 at 350 °C) 10% Mo-ηAl_2O_3 samples were axially symmetric. They found that the best fit for the outgassed sample was achieved by using a Lorentzian line shape whereas a Gaussian line shape provided the best fit for the reduced sample.

The components of the **g** tensor also provide information on the environment of the Mo(V) species, and this will be the subject of the following section.

(*d*) *Mo(V) Environment.* The host alumina is a spinel with many defects whose surface structure has open octahedral and tetrahedral sites. Sites of lower symmetry are also possible. Thus, the Mo(V) species could exhibit ESR spectra which are totally symmetric, axially symmetric, or totally asymmetric, depending on the particular lattice site it occupies. In earlier work we had shown that our results were consistent with the Mo(V) species occupying a tetragonally distorted octahedral site.[16] It has also been argued that the origin of the same signal cold be ascribed to Mo(V) in tetragonally distorted tetrahedral symmetry.[21,22]

Several authors have addressed the question of extracting precise components of the **g** tensor and relating them to the environment of the Mo(V).[14,16,18] In order to observe ESR signals, the orbital degeneracy of the d^1 level [Mo(V)] must be removed by the crystal field. If we accept the tetragonally distorted octahedral site of Mo(V) (since symmetry considerations will not distinguish it from the tetragonally distorted tetrahedral site), then the g component parallel to the field direction ($g_\parallel$) and the g component perpendicular to the field direction ($g_\perp$) can be related to the energy level splitting as follows:[14,16,18]

$$\frac{g_e - g_\perp}{g_e - g_\parallel} = 1/4\left(\frac{\Delta}{\delta}\right) = \frac{1}{\alpha}$$

where g_e is the g value of a free electron, Δ is the energy difference between $^2B_1$ and $^2B_2$, δ is the difference between ^2E and $^2B_2$, and $1/\alpha$ is simply the quotient as shown in the above equation. This quotient can be used as a quantitative, empirically derived measure of the degree of distortion of the Mo(V) site. Earlier measurements[16] had shown some variation in the $1/\alpha$ parameter with the type of treatment of the molybdena-alumina system. Table VI shows both additional measurements of the molybdena-alumina system as well as a literature survey of ESR data of Mo(V) in various hosts and in solution. It is clear from this table that the immediate environment of the Mo(V) species varies greatly depending on the host material. The value of Δg was found to vary from 0.093 to 0.028, corresponding to a variation of $1/\alpha$ values from 0.337 to 0.703. Note that the Δg and $1/\alpha$ values describing the various molybdena/alumina systems fall in a narrow range on this spread of values. The $Mo(CO)_6$-SiO_2 system[28] is a particularly dramatic example. Before any thermal treatment, the signal is almost totally isotropic ($\Delta g = 0.039$). However, after thermal treatments, the Mo(V) environment is distorted considerably with $\Delta g = 0.093$. The data in this table also hint at the following interesting possibility. If a given crystal field environment were desirable, it could be achieved by choosing a priori the proper treatments and support. What remains to be tested is which of the different (Mo(V) environments is best correlated with different catalytic reactions.

IV. Discussion and Conclusions

In the previous sections we have presented and discussed experiments in which we attempted to systematically develop data that would allow an understanding of the molybdenum species in a molybdena-alumina system. Through physical characterizations, XPS and ESR measurements, we have studied the effects on this system of the following: (a) support, (b) thermal treatments, and (c) adsorption of organics with which the surface may undergo electron-transfer reactions. The key points that emerge from this study are now presented.

(*a*) *Distribution of Molybdenum Valences.* The data presented clearly indicate that the experimental variations have important effects on the properties of the molybdena-alumina system. These same data also attest to the great complexity of this system. Although the starting material for the preparation of the catalyst, MoO_3, contained only Mo(VI), molybdenum was also found to exist in other lower valences when incorporated in alumina. XPS determined that the surface layers of the 9% Mo-

ηAl_2O_3 samples contained mixtures of Mo(IV), -(V), and -(VI), and ESR measurements detected the Mo(V) species in these samples. Neither technique detected the Mo(III) species which has been postulated to be important in certain applications of the molybdena–alumina system (e.g., hydrodesulfurization reactions).

(b) *Support Effects.* It appears that the support is critical in determining the distribution of molybdenum valences in this system. Namely, ESR does not detect any Mo(V) in unsupported molybdena samples of MoO_2 or MoO_3. On the other hand, XPS detected Mo(IV), and Mo(VI) in unsupported MoO_2 and only Mo(VI) in unsupported MoO_3. The presence of the Mo(VI) species in the MoO_2 standard has been attributed to surface oxidation of the sample.

(c) *Thermal Treatment of 9% Mo–ηAl_2O_3.* Thermal treatments also had dramatic effects on the 9% Mo–ηAl_2O_3 samples. A Mo(V) ESR species was not observed in thermally untreated 9% Mo–ηAl_2O_3 samples, and Howe and Leith[28] also reported that Mo(V) ESR signals were not detected in molybdena–alumina catalysts unless the samples had undergone a prolonged 16-h evacuation at room temperature. However, we have always detected the Mo(V) ESR species in 9% Mo–ηAl_2O_3 samples which had been thermally treated, either by evacuation and calcination or by H_2 reduction. Note that the addition of aromatics, heteroaromatics, or solvent is not required for Mo(V) formation and detection by ESR (Table III). The maximum Mo(V) detected in thermally treated 9% Mo–ηAl_2O_3 samples by ESR techniques is 6.4×10^{18} spins/g of catalyst or 1.3% of the total molybdenum incorporated into the catalyst. Comparable results were previously obtained by Seshadri and Petrakis.[16] The ESR results show that thermal treatments produce some Mo(V) but that the *type* of thermal treatment is not important in the overall production of this species. From XPS analysis, the surface composition of 9% Mo–ηAl_2O_3 (without thermal treatment) is shown to be entirely Mo(VI), which is in agreement with the ESR results (Table III). The various thermal treatments of the molybdena–alumina system, however, produced radically different surface compositions, depending on the *type* of thermal treatments used.

(d) *Types of Thermal Treatment of 9% Mo–ηAl_2O_3 Samples.* An ESR analysis of samples which had been prepared by the same types of thermal treatments (2-h EC and 4-h EC) demonstrated that the *longer* heating time resulted in a *decreased* Mo(V) ESR signal intensity (Table III). This variation of ESR signal intensities is in agreement with earlier work by Seshadri and Petrakis[16] and by Patterson and co-workers.[8] A variation in Mo(V) signal intensities between these two groups of EC samples could not be detected by XPS, however. As stated earlier, the XPS spectra of most EC samples contained almost exclusively the Mo(VI) species. Small Mo(V) signals may also be present but could not be quantified by XPS.

The differences between the two *types* of thermal treatments, i.e., EC and H_2 Red., were also reflected in samples analyzed by both techniques. ESR analysis showed that the Mo(V) concentration in H_2 Red. samples was nearly constant compared with the Mo(V) concentration in EC samples which varied as a function of both heating time and probes added. XPS results also indicated a difference between the two *types* of thermal treatments, but on a much larger scale. Although the surface composition of EC samples consisted mainly of Mo(VI), about half of the surface Mo(VI) in H_2 Red. samples was reduced to Mo(V) and Mo(IV) valences. These XPS results were determined by deconvolution of the XPS Mo 3d envelopes.

(e) *ESR Spectral Features of Thermally Treated 9% Mo–ηAl_2O_3.* A comparison of ESR spectral parameters (other than spin concentrations) provided evidence that the different thermal treatments produced different structural environments for the Mo(V) species. Regardless of the particular aromatic or heteroaromatic probe used, the variation in signal intensities, g values, and line widths among the H_2-reduced samples was less than half of that observed among samples from either of the evacuation and calcination procedures (2- or 4-h). The spectral shape of the H_2 Red. Mo(V) ESR signals was also quite distinct from that of the EC samples. Spectral simulations showed that although both EC and H_2 Red. Mo(V) signals were axially symmetric, the best fit for a representative EC spectrum was provided by a Gaussian line shape with $\Delta H_{pp} = 25$ G and $\Delta g = 0.0457$. A typical H_2 Red. spectrum required a Lorentzian line shape with $\Delta H_{pp} = 48$ G and $\Delta g = 0.0345$. Thus, the hydrogen-reduced spectra are generally broader and more symmetric than evacuation and calcination samples and, somewhat surprisingly, require Lorentzian line shapes for best fit. In neither case did the computer simulation give a perfect fit for the entire signal. The discrepancies were most apparent in the tail of the signal. This fact is not inconsistent with the existence of a range of Mo sites with varying environments.

In conclusion, our study of this important model catalyst system has shown that both the support and the various thermal treatments play a critical role. ESR and XPS analyses have demonstrated that these factors determine not only the distribution of molybdenum valences but also their environments. ESR provided information on the concentration of the Mo(V) species in the bulk catalyst and also on the crystal field of this molybdenum species. XPS studies of the catalyst surface determined the distribution of Mo(IV), -(V), and -(VI). XPS and ESR results compliment each other in many instances although there still remain discrepancies in the quantitative comparison of results from the two techniques. This disagreement needs to be resolved by careful studies of the same systems using both techniques.

References and Notes

(1) G. C. A. Schuit and B. C. Gates, *AIChE J.*, **19**, 417 (1973), and references therein.
(2) B. C. Gates, J. R. Katzer, and G. C. A. Schuit, "Chemistry of the Catalytic Process", McGraw-Hill, New York, 1979, and references therein.
(3) F. E. Massoth, *J. Catal.*, **30**, 204 (1973), and references therein.
(4) "Molybdenum Catalyst Bibliography (1973 & 1974)", Supplement No. 4, compiled by F. C. Wilhelm, Climax Molybdenum Co. of Michigan, Inc.
(5) "Molybdenum Catalyst Bibliography (1975 & 1976)", Supplement No. 5, compiled by W. W. Swanson, Climax Molybdenum Co. of Michigan, Inc.
(6) W. E. Swartz, Jr., and D. M. Hercules, *Anal. Chem.*, **43**, 1774 (1971).
(7) A. Cimino and B. A. DeAngelis, *J. Catal.*, **36**, 11 (1975).
(8) T. A. Patterson, J. C. Carver, D. E. Leyden, and D. M. Hercules, *J. Phys. Chem.*, **80**, 1700 (1976).
(9) R. I. Declerck-Grimee, P. Canesson, R. M. Friedman, and J. J. Fripiat, *J. Phys. Chem.*, **82**, 885 (1978).
(10) G. K. Boreskov, V. A. Dzis'ko, V. M. Emel'yanova, Y. I. Pechnerskaya, and V. B. Kazanskii, *Dokl. Akad. Nauk SSSR*, **150**, 829 (1963).
(11) J. Masson and J. Nechtschein, *Bull. Soc. Chim. Fr.*, 3933 (1968).
(12) K. S. Seshadri and L. Petrakis, *J. Phys. Chem.*, **74**, 4102 (1970).
(13) K. S. Seshadri, F. E. Massoth, and L. Petrakis, *J. Catal.*, **19**, 95 (1970).
(14) M. Dufaux, M. Che, and C. Naccache, *J. Chim. Phys. Phys.-Chim. Biol.*, **67**, 527 (1970).
(15) C. Naccache, J. Bandiera, and M. Dufaux, *J. Catal.*, **25**, 334 (1972).
(16) K. S. Seshadri and L. Petrakis, *J. Catal.*, **30**, 195 (1973).
(17) L. Burlamacchi, G. Martini, F. Trifiro', and G. Caputo, *J. Chem. Soc., Faraday Trans. 1*, **71**, 209 (1975).
(18) L. Burlamacchi and G. Martini, "Application of the ESR Technique to the Olefin Oxidation by Molybdate Catalysts", presented at the Czechoslovack–Italian Symposium on Catalysis, Prague, Oct 1976.
(19) M. Che, F. Figueras, M. Forissier, J. McAteer, M. Perrin, J. L. Portefaix, and H. Praliaud, "Influence of the Symmetry of the Molybdenum Ion on the Selectivity for Propylene Oxidation", presented at the 6th

International Congress on Catalysis, London, July 1976.
(20) W. K. Hall and M. Lo Jacono, "The Surface Chemistry of Molybdenum–Alumina Catalysts", presented at the 6th International Congress on Catalysis, London, July 1976, paper A-16.
(21) S. Abdo, R. B. Clarkson, and W. K. Hall, *J. Phys. Chem.*, **80**, 2431 (1976).
(22) S. Abdo, M. Lo Jacono, R. B. Clarkson, and W. K. Hall, *J. Catal.*, **30**, 330 (1975).
(23) The program was written by Dr. Paul H. Kasai of Union Carbide and was made available by Dr. David W. Pratt of the University of Pittsburgh. The plotting routine was modified, and several input requirements were added in order to fit our needs.
(24) P. Ratnasamy, *J. Catal.*, **40**, 137 (1975).
(25) F. Lepage, P. Baillaif, and J. Bardolle, *C. R. Hebd. Seances Acad. Sci., Ser C*, **280**, 1089 (1975).
(26) K. S. Kim, W. L. Baitinger, J. W. Amy, and N. Winograd, *J. Electron Spectrosc. Relat. Phenom.*, **5**, 351 (1974).
(27) F. Campadelli and J. C. J. Bart, *React. Kinet. Catal. Lett.*, **3**, 435 (1975).
(28) R. F. Howe and I. R. Leith, *J. Chem. Soc., Faraday Trans. 1*, **69**, 1967 (1973).
(29) P. F. Cornaz, J. H. C. Van Hooff, F. J. Pluijm, and G. C. A. Schuit, *Faraday Discuss. Chem. Soc.*, **41**, 290 (1966).
(30) G. Martini, *J. Magn. Reson.*, **15**, 262 (1974).
(31) M. Dufaux, M. Che, and C. Naccache, *C. R. Hebd. Seances Acad. Sci., Ser. C*, **248**, 2255 (1969).
(32) A. S. Sultanov, K. A. Samigov, G. Sh. Talipov, and N. Sh. Inoyatov, *Kinet. Katal.*, **12**, 1579 (1971).
(33) G. Sperlich, P. Urban, and G. Frank, *Z. Phys.*, **263**, 315 (1973).
(34) L. Burlamacchi, G. Martini, and E. Ferroni, *J. Chem. Soc., Faraday Trans. 1*, **68**, 1586 (1972).
(35) N. S. Garif'yanov and V. N. Fedotor, *Zh. Strukt. Khim.*, **3**, 711 (1962).
(36) M. M. Abraham, J. P. Abriata, M. E. Foglio, and E. Pasquini, *J. Chem. Phys.*, **45**, 2069 (1966).

ESR Investigation of Radical Cations Formed from Aromatics and Heteroaromatics Adsorbed on Mo–Al_2O_3 Surfaces

L. Petrakis,* P. L. Meyer, and Gerald L. Jones

Gulf Research and Development Company, Pittsburgh, Pennsylvania 15230 *(Received September 27, 1979)*

Publication costs assisted by Gulf Research and Development Company

Molybdena–alumina is an important model catalyst system that has attracted considerable attention over the years. The behavior of adsorbed species on catalytic surfaces is also of interest because this may lead to a better understanding of the reaction mechanisms involved in the catalytic process. Using electron spin resonance, we have continued our systematic study of the molybdena–alumina system to which various aromatics and heteroaromatics have been added. We have investigated electron-transfer reactions with the molybdena–alumina surface and have also investigated the structural and dynamical aspects of the resulting adsorbed cations. Computer fitting of the cation ESR spectra has been carried out for a more precise determination of spectral parameters, and a comparison with solution spectral parameters has also been made.

I. Introduction

The molybdena–alumina system is a chemically interesting model of many industrially significant catalysts, and as a result, it has received considerable attention.[1–5] The incorporation of molybdena in the alumina support and subsequent thermal treatments can effect significant changes in the solid-state and surface properties of the system. For example, it is quite well-known that molybdena, even though it is incorporated initially as a hexavalent species, shows a distribution of valences, the distribution being determined by the thermal history of the system.[6–8] In addition, the surface acidity of the support is changed significantly by the molybdenum deposit, the changes being manifested by the radically different appearance of the IR[9] and NMR[10] spectra of adsorbed pyridine. Finally, the molybdena–alumina surface is sufficiently different from the alumina support to allow the former to enter readily into electron-transfer reactions with organic molecules that are adsorbed on its surface. These electron-transfer reactions result in the formation of radical cations which may be studied by electron spin resonance (ESR) techniques.[11–19] The radical cations are, thus, sensitive probes of the surface of the model system and of the changes it undergoes with the various treatments.

In this paper we report ESR results which extend earlier measurements on the radical ions formed on the surface of molybdena–alumina.[14,15] A carefully selected series of aromatic and heteroaromatic molecules was used to probe the surface characteristics of a Mo–ηAl_2O_3 system. The molecules contained one, two, or three aromatic rings with greatly varying structural characteristics and ionization potentials. The ESR study of these species allows us not only to systematically investigate their electron-transfer reactions with the surface but also to assess the structural and dynamical aspects of the resulting adsorbed cations. The Mo(V) ESR spectra of the substrate have also been monitored, thus allowing for a more definitive assessment of the electron-transfer processes between probe molecules and catalytic surfaces. The precise ESR spectral parameters of the radical ions, obtained from computer fitting of the experimental spectra, are compared to the corresponding parameters of the solution species.

II. Experimental Section

A. Preparation of Samples. The experimental procedures used have been described earlier in detail.[20] Batches of 9% (by weight) Mo–ηAl_2O_3 were prepared, pelletized, and sieved to 20–40 mesh size. The solid-state and surface characteristics of this model catalytic system were investigated by monitoring the structure and dynamical behavior of certain aromatics and heteroaromatics ("probes") adsorbed on the catalyst surface. Fifteen different one-, two-, or three-ring aromatic hydrocarbons, some of which contained N, O, or S heteroatoms, were investigated (Figure 1). Solutions 10^{-2} M of the aromatic or heteroaromatic in cyclohexane were added to the catalyst. On

0022-3654/80/2084-1029$01.00/0